NUREG/CR-3878
BNL-NUREG -51797

MODELING CONSIDERATIONS FOR THE PRIMARY SYSTEM OF THE EXPERIMENTAL BREEDER REACTOR-II

I.K. Madni

Date Published — June 1984

CODE DEVELOPMENT, VALIDATION AND APPLICATION GROUP
DEPARTMENT OF NUCLEAR ENERGY, BROOKHAVEN NATIONAL LABORATORY
UPTON, NEW YORK 11973

Prepared for the U.S. Nuclear Regulatory Commission
Office of Nuclear Regulatory Research
Contract No. DE-AC02-76CH00016

NUREG/CR-3878
BNL-NUREG-51797
AN

MODELING CONSIDERATIONS FOR THE PRIMARY SYSTEM OF THE EXPERIMENTAL BREEDER REACTOR-II

I.K. Madni*

*Visiting Scientist from the Department of Mechanical Engineering
University of Petroleum & Minerals, Dhahran

Manuscript Completed — May 1984
Manuscript Published — June 1984

DEPARTMENT OF NUCLEAR ENERGY
BROOKHAVEN NATIONAL LABORATORY
UPTON, LONG ISLAND, NEW YORK 11973

PREPARED FOR
OFFICE OF NUCLEAR REGULATORY RESEARCH
U.S. NUCLEAR REGULATORY COMMISSION
WASHINGTON, D.C. 20555
FIN NO. A-3015

Available from
GPO Sales Program
Division of Technical Information and Document Control
U.S. Nuclear Regulatory Commission
Washington, D.C. 20555
and
National Technical Information Service
Springfield, Virginia 22161

ABSTRACT

This report describes the additional heat transfer and coolant dynamic models for components and processes, that are needed for simulation of the primary system of the Experimental Breeder Reactor-II (EBR-II). This work forms part of the Super System Code (SSC) application efforts to provide predictions of EBR-II overall plant behavior.

TABLE OF CONTENTS

LIST OF FIGURES

NOMENCLATURE

Symbol	Description	Unit
A	Cross-sectional area or heat transfer area	m^2
C	Specific heat capacity	J/kg-K
D	Diameter	m
e	Specific enthalpy	J/kg
g	Gravitational acceleration	m/s^2
Gr	Grashoff number	--
H	Pump head	m
h	Film heat transfer coefficient	W/m^2-K
K	Loss coefficient	--
k	Thermal conductivity	W/m-K
L	Length of pipe section	m
L,ℓ	Length	m
M,m	Mass	kg
N	Number of nodes in a pipe run or IHX section	--
N_s	Specific speed of pump	--
Nu	Nusselt number	--
P	Pressure	N/m^2
Pr	Prandtl number	--
Q	Heat transfer rate	W
Ra	Rayleigh number (RePr)	--
Re	Reynolds number ($WD/A\mu$)	--
T	Temperature	K
t	Time	s
U	Overall heat transfer coefficient	W/m^2-K
V	Volume	m^3
W	Mass flow rate	kg/s
x	Axial coordinate	m
z	Vertical distance	m
z_{cp}	Cold pool free surface level	m
Δ	Difference or loss	--
μ	Dynamic viscosity	$N-s/m^2$
ν	Kinematic viscosity	m^2/s
ρ	Coolant density	kg/m^3

NOMENCLATURE (Cont'd)

Subscript	Description
C	Core flow
cg	Cold pool to cover gas
CP	Cold pool value
cw	Coolant to wall
f	Friction
f,g	Friction, Gravity, etc.
g	Cover gas value
i	Value at nodal point i
in	Inlet
j	Index denoting channel number in core
Na	Sodium
o	Outlet
P	Pump value
p	At constant pressure
Pin	Pump inlet
Po	Pump outlet
ws	Wall to outside surface of sleeve
sCP	Outside surface to cold pool
R	Rated value
Rin	Reactor inlet
Ro	Reactor outlet
w	Wall
X	IHX value
x	Coordinate in flow direction
Xo	IHX outlet

ACKNOWLEDGMENT

The author is indebted to M. Khatib-Rahbar for numerous technical discussions and his invaluable assistance during this study. The author also wishes to extend his appreciation to J. G. Guppy for his active cooperation and support of this work, to E. G. Cazzoli for providing information on the current status of SSC, and to G. J. Van Tuyle for providing on loan a copy of the System Design Description of EBR-II. Thanks are also due to J. G. Guppy, M. Khatib-Rahbar, and R. J. Cerbone for reviewing the report and to C. Falkenbach for typing the manuscript.

1. INTRODUCTION

The Experimental Breeder Reactor II (EBR-II) is an experimental LMFBR power plant of pool design, located in Idaho, and rated to produce 62.5 MW thermal power (20 MWe). The mission of EBR-II has evolved to the point where, together with serving as an irradiation facility for fuels and materials, it is being extensively used to provide experimental in-plant test data on the thermal, hydraulic, and neutronic response of the core and plant to normal and abnormal operation. These tests have, and will continue to provide very useful information for the future design, operation and safety analysis of LMFBR plants. For example, the test data can form the basis for validation or further development of models intended to predict plant behavior during a variety of operating conditions.

The work presented in this report is in support of the Super System Code (SSC) application efforts to provide predictions of EBR-II overall plant behavior. This report describes the models required to represent the EBR-II primary system. The discussion will focus only on new models and modifications required due to some special design features in EBR-II, beyond the models already present in SSC [1].

SSC is designed to enable simulation of all plant-wide transients that may be required in safety evaluation. These include a variety of transients ranging from normal operational maneuvers to upset conditions caused by loss of flow or reactor power changes.

The immediate application for the models to be described, as part of SSC, is to simulate the current series of whole-plant type transients, including natural circulation, that are being planned to be performed on the EBR-II plant beginning in 1984. The comparisons thus obtained will also contribute towards the validation of SSC as a plant simulation tool.

After a brief description of the EBR-II primary system in Chapter 2, a comprehensive discussion of heat transfer and coolant dynamic models is provided in Chapter 3. Finally, Chapter 4 presents the EBR-II steady-state operating data and physical (dimensional) data on individual components and the overall primary system.

2. PRIMARY SYSTEM DESCRIPTION

Figure 1 [2] is a schematic diagram of the EBR-II primary heat transport system. From this figure, it is clear that EBR-II is of the pool design in which all the primary components including reactor, pumps, intermediate heat exchanger, piping, as well as shutdown coolers, and other support systems are submerged in a large pool of sodium, contained within the primary tank. The space between the sodium free surface and primary tank is filled with argon gas. The primary tank is of double-wall construction (tank within a tank), the space between the inner and outer tanks being filled with inert gas. The outer tank is heavily insulated to minimize heat loss from the primary system.

The reactor is centrally located at the bottom of the primary tank, with the pumps and heat exchanger arranged radially around the reactor and elevated somewhat above it. The reactor consists of a hexagonal shaped central core, containing enriched uranium, surrounded by radial and axial blankets, containing either depleted uranium, or stainless steel. The subassemblies are contained in and supported by a stainless steel reactor vessel, comprised of a grid plenum assembly, reactor vessel shell, and reactor vessel cover, and surrounded by a radial neutron shield. The vessel top cover, which also contains neutron shielding, is removable to permit fuel handling. It contains penetrations for entry of control rod drive shafts, special in-core test facilities, etc. During power operation, a small amount of leakage occurs through various openings in the cover. This leakage flow is employed as a part of the neutron shield cooling system in this region.

Forced flow to the reactor is provided by two main sodium pumps, which are vertically mounted, single-stage, centrifugal units, operating in parallel, each rated at a maximum of approximately 0.35 m^3/s at 61 m head. Each impeller is submerged in primary sodium; however, the motor units are located outside the primary tank. Primary system flow is varied by manually adjusting the pump speeds.

An auxiliary electromagnetic pump of small capacity and low head operates in series with the large primary pumps. During normal operation, the auxiliary pump has no appreciable effect on the primary coolant flow. The main

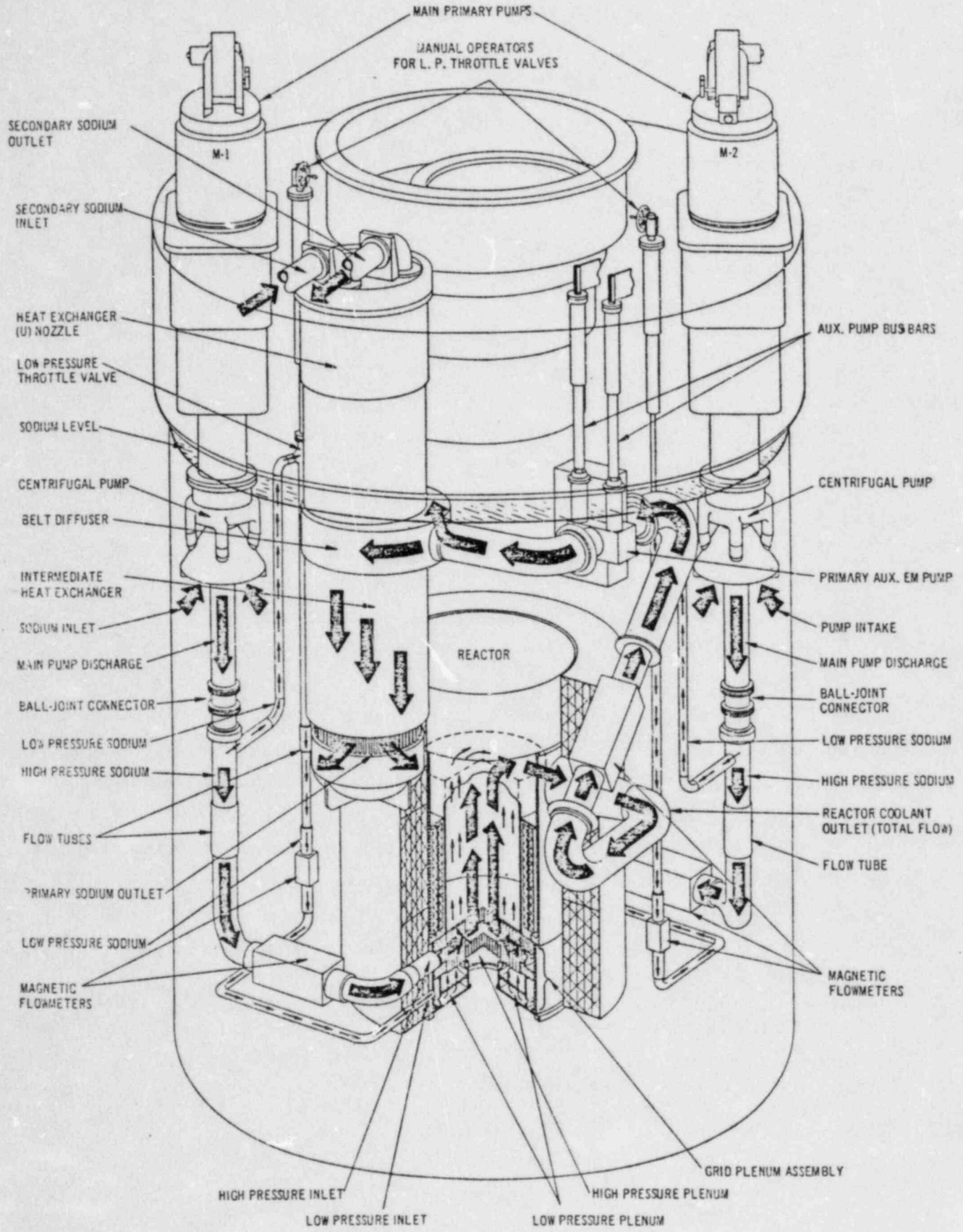

Fig. 1 EBR-II Primary Heat Transport System [2]

purpose of this pump is to augment thermal convection under certain conditions of reactor shutdown. The reactor outlet piping carries hot sodium through the environment of the cold pool, at substantially lower temperature. It is therefore provided with an insulating steel sleeve, surrounding the pipe, to minimize heat losses. The space between pipe wall and sleeve is filled with stagnant sodium from the pool.

The IHX transfers essentially all of the heat generated in the reactor to the secondary system. It is a single-pass counter flow exchanger. Primary sodium (radioactive) enters the exchanger via piping, flows downward around the tubes on the shell side, and returns to the primary tank through a cylindrical opening near the bottom. The secondary sodium (non-radioactive) flows upward through the tubes. To minimize pressure drop in the unit, axial flow is maintained as much as possible. The IHX primary outlet is located above the reactor centerline to provide natural convection shutdown cooling.

The coolant flow path is as follows: sodium from the primary tank enters the pumps through sump-type inlets, and exits into a main pipe where it is divided into high and low pressure streams. High pressure sodium is piped from each pump outlet directly to the high-pressure inlets of the reactor grid-plenum assembly and flows upward through the core and inner blanket assemblies (inner core region). The control and safety rods, located in the inner core region are also cooled by the high pressure coolant. Low pressure coolart is routed via a smaller line through a throttle valve, to the low-pressure inlets of the grid-plenum assembly, and flows upward through the outer blanket assemblies. Both streams mix in the reactor outlet plenum. The mixed coolant exits the reactor vessel through a single outlet nozzle, flows via piping, through the auxiliary EM pump, and into the shell side of the IHX where it is cooled and returns to the primary tank at nearly the bulk pool sodium temperature.

Leakages occur at several points along the coolant flow path. These are presented in Chapter 4.

3. ANALYTICAL MODELS

3.1 Tank Energy Balance

The components of the primary system required for energy balance are shown in Fig. 2. The coolant exiting the core flows via piping to the IHX. A large temperature gradient exists across the pipe wall, causing some heat losses to the tank sodium. Cooled sodium from the IHX mixes with the sodium in the pool, and sodium leaves the pool via the pump inlets. Heat losses from the reactor outlet plenum walls and piping, to the tank sodium, need to be included in the energy balance. Leakages to the bulk sodium occur at pump disconnects, throttle valves, reactor grid-plenum, reactor vessel cover, and IHX inlet. Of these, the energy addition to tank sodium due to leakages at the reactor vessel cover and IHX inlet, are expected to be significant. The remaining leakages occur at nearly the temperature of the cold pool and, even though included in the analysis, are not expected to be significant. Other extraneous losses include the heat lost to the shutdown cooler, if operative. There is also heat transfer between the pool sodium and cover gas, and between cover gas and roof structure. The outer surface and roof of the primary tank, are assumed perfectly insulated. This assumption is justified due to the heavy shielding and insulation surrounding these structures [2].

Allowances are made in the formulation for the possibility that some part of the IHX flow can directly stream into each adjacent pump suction without mixing with the cold pool sodium. This is done through user-specified bypass fractions β_{X1} and β_{X2}. Specifying two bypass fractions allows the behavior of the entering flow to be different for each pump, depending on its location relative to the IHX outlet. The rest of the IHX flow is assumed to mix completely with the pool sodium.

Based on the above considerations, energy equations are written as follows:

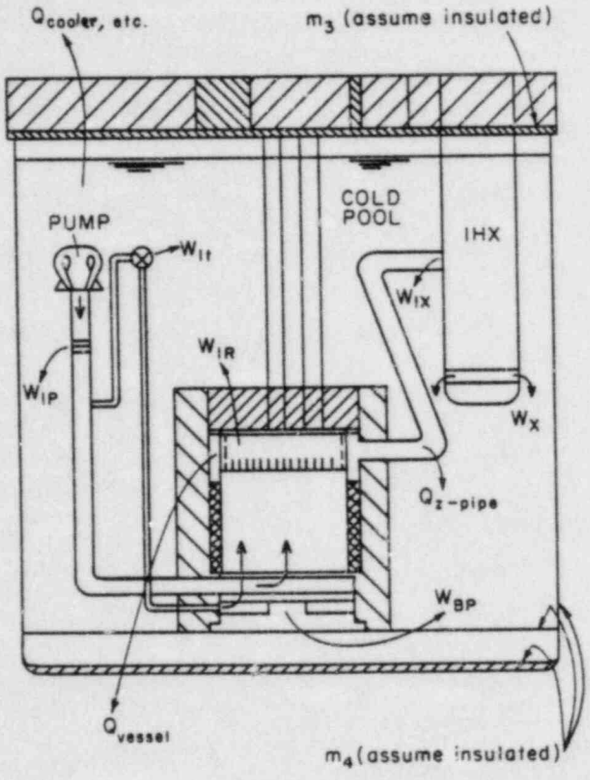

Fig. 2 Primary System Configuration for Tank Energy Balance

Cold pool

$$(\rho V)_{CP} \frac{de_{CP}}{dt} = (1 - \beta_{X1} - \beta_{X2}) W_X (e_{Xo} - e_{CP}) + W_{\ell R} (e_{Ro} - e_{CP})$$

$$+ W_{BP} (e_{Rin} - e_{CP})$$

$$+ Q_{Z\text{-pipe}} + Q_{Vessel} - U_{cg} A_{cg} (T_{CP} - T_g)$$

$$- (UA)_{cm4} (T_{CP} - T_{m4}) - Q_{cooler,etc} \qquad (3\text{-}1)$$

Here, $Q_{Z\text{-pipe}}$ is obtained as the sum of heat losses calculated for all the nodes in the model for reactor outlet pipe (see Section 3.2). Q_{vessel} is obtained from energy balance model of the reactor outlet plenum, allowing for heat losses to the pool sodium. $Q_{cooler,etc}$ represents other extraneous losses, including heat removal at the shutdown cooler(s), if operating.

Lower structures (metal m4)

$$(MC)_{m4} \frac{dT_{m4}}{dt} = (UA)_{cm4} (T_{CP} - T_{m4}) \qquad (3\text{-}2)$$

Here, m4 is taken to be the mass of primary tank and core support structures in contact with cold pool sodium.

Cover gas

$$(MC)_g \frac{dT_g}{dt} = (UA)_{cg} (T_{CP} - T_g) - (UA)_{gm3} (T_g - T_{m3}) \qquad (3\text{-}3)$$

Her , m3 is taken to be the mass of roof and the part of primary tank wall in contact with the cover gas.

Due to the possibility of short-circuiting, the enthalpy of coolant exiting the pumps is not necessarily equal to the enthalpy of the cold pool sodium plus the pump enthalpy rise (Δe_p). Rather, it is given by:

$$(\rho V)_{P1} \frac{d\, e_{P1o}}{dt} = (W_1 - \beta_{X1} W_X)(e_{CP} - e_{P1o}) + \beta_{X1} W_X (e_{Xo} - e_{P1o}) + \Delta e_{P1} \quad (3\text{-}4)$$

$$(\rho V)_{P2} \frac{d\, e_{P2o}}{dt} = (W_2 - \beta_{X2} W_X)(e_{CP} - e_{P2o}) + \beta_{X2} W_X (e_{Xo} - e_{P2o}) + \Delta e_{P2} \quad (3\text{-}5)$$

where W_1, W_2 are the mass flow rates through pumps 1 and 2, respectively.

3.2 Reactor Outlet Pipe

Since a substantial temperature gradient equal to the difference between reactor outlet and inlet temperatures exists between the hot sodium in this pipe and the cold pool, the heat losses from here to the bulk sodium are much more significant than for the cold leg piping. Figure 3 shows the model configuration for energy balance.

In the axial direction, the number of nodal interfaces (N) is user-specified, the number being influenced by the pipe length and the coolant velocity at full flow. In the radial direction, there are four nodes - coolant, composite pipe wall including part of stagnant sodium, outer surface of insulating sleeve, and cold pool sodium. As shown in the figure, the locations of coolant and wall temperatures form a staggered arrangement.

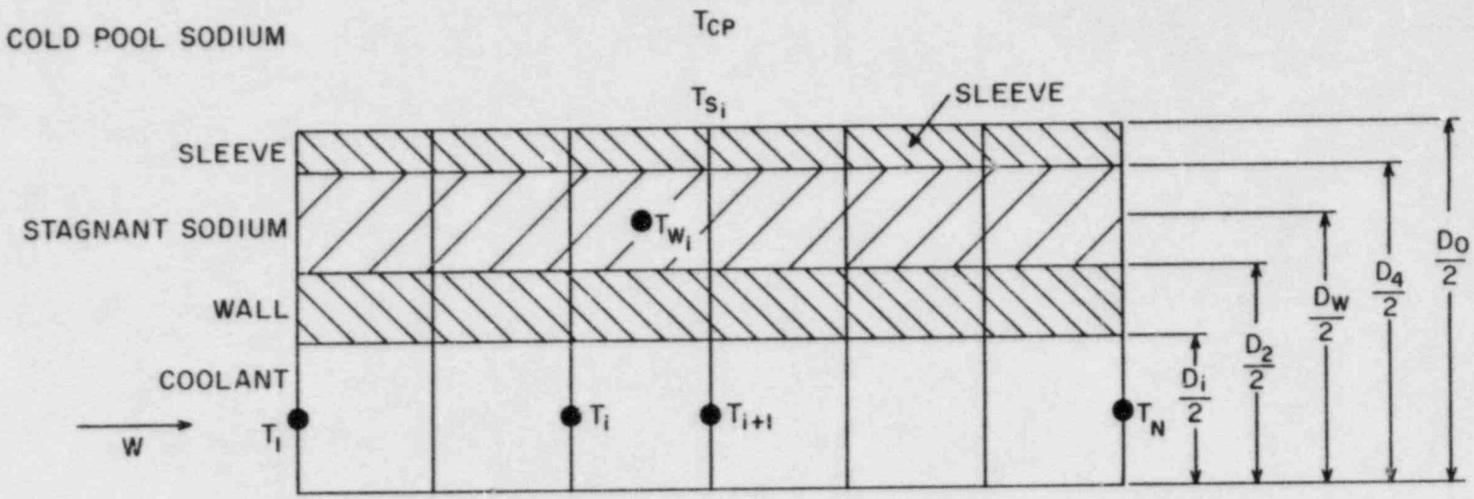

Fig. 3 Model Configuration for Energy Balance in Reactor Outlet Pipe

3.2.1 Governing Equations

The governing equations are obtained by the nodal heat balance method. Energy balance is applied over the control volume formed between two adjacent fluid nodal interfaces to obtain the coolant equation. The wall equation is related to the coolant equation through the heat flux term. These equations can be written for i = 1, N - 1, as follows:

Coolant

$$\rho_{i,i+1} A\Delta x \frac{de_{i+1}}{dt} = W(e_i - e_{i+1}) - U_{cw} A_{cw} [T_{i,i+1} - T_{wi}] \qquad (3\text{-}6)$$

where e_{i+1} is the coolant enthalpy at the nodal interface i+1, $T_{i,i+1}$ is the average coolant temperature in the control volume between interfaces i and i+1, expressed as

$$T_{i,i+1} = \frac{T_i + T_{i+1}}{2}$$

$\rho_{i,i+1}$ is the coolant density corresponding to $T_{i,i+1}$, W is the flow rate in the pipe, A is the cross-sectional area for flow given by $\pi D^2_i/4$, U_{cw} is the overall heat transfer coefficient between coolant and wall, evaluated at the midpoint between coolant nodal interfaces i and i+1, and A_{cw} is the area for heat transfer between coolant and wall, given by

$$A_{cw} = \pi D_i \Delta x.$$

Inherent in Equation (3-6) is the assumption that

$$\frac{de_i}{dt} \approx \frac{de_{i+1}}{dt} \approx \frac{de_{i,i+1}}{dt}$$

Composite wall

$$M_w C_{wi} \frac{dT_{wi}}{dt} = U_{cw} A_{cw} [T_{i,i+1} - T_{wi}] - U_{ws} A_{ws} [T_{wi} - T_{si}] \qquad (3\text{-}7)$$

where

$$M_w C_{wi} = (M_{pipe}C_{pipe} + M_{Na}C_{Na} + M_{sleeve}C_{sleeve}).$$

Outer surface

$$U_{ws} A_{ws} [T_{wi} - T_{si}] = (hA)_{sCP} [T_{si} - T_{CP}]. \quad (3\text{-}9)$$

Here, A_{ws} is taken to be the outside surface area of the sleeve. Based on this selection for A_{ws}, we have

$$A_{ws} = A_{sCP} = \pi D_o \Delta x.$$

3.2.2 Heat Transfer Coefficients

In Eqs. (3-6) through (3-9), the overall heat transfer coefficients U_{cw} and U_{ws} are defined based on the resistance concept as

$$\frac{1}{U_{cw}} = \frac{1}{h_i} + \frac{D_i}{2k_w} \ln\left(\frac{D_2}{D_i}\right) + \frac{D_i}{2k_{Na}} \ln\left(\frac{D_w}{D_2}\right) \quad (3\text{-}10)$$

$$\frac{1}{U_{ws}} = \frac{D_o}{2k_{Na}} \ln\left(\frac{D_4}{D_w}\right) + \frac{D_o}{2k_w} \ln\left(\frac{D_o}{D_4}\right) \quad (3\text{-}11)$$

where D_i, D_2, D_w, D_4, D_o are the diameters indicated in Fig. 3. The film heat transfer coefficient h_i is given in terms of Nusselt number correlations presented in [3].

In Eq. (3-9), h_{sCP} (= $Nu_o\ k_{CP}/D_o$) represents the film heat transfer coefficient between the outer surface of the sleeve and the bulk pool sodium, and can be obtained by using certain established correlations for Nu for a cylinder immersed in liquid metal. The form of the Nu correlation is seen to be rather insensitive to the geometry, whether flat plate or circular cylinder, as long as the characteristic dimension is appropriately selected.

For laminar flow, we select the correlation recommended for a horizontal cylinder in liquid as follows [4]:

$$Nu = 0.66 \left[\frac{Gr\ Pr^2}{0.953 + Pr} \right]^{0.25} \qquad (3\text{-}12)$$

For $Pr \rightarrow 0$, this reduces to

$$Nu = 0.69 Ra^{0.25}\ Pr^{0.25} \qquad Ra \leq 10^8 \qquad (3\text{-}13)$$

Here, Ra = GrPr, and

$$Gr = \frac{g\beta D^3 \Delta T}{\nu^2} \qquad (3\text{-}14)$$

where ΔT is the temperature difference between sleeve surface and cold pool, i.e., $[T_S - T_{CP}]$, ν is the kinematic viscosity ($= \mu/\rho$) and β is the coefficient of the thermal expansion of sodium $\left(= -\frac{1}{\rho}\left(\frac{\partial \rho}{\partial T}\right)_p \right)$. The coolant properties are evaluated at film temperature, $T_f = (T_S + T_{CP})/2$.

For turbulent flow, the equation used in SSC-P for a vertical plate is suggested [5]:

$$Nu = 0.025\ Pr^{0.467}\ Gr^{0.4} \qquad Ra > 10^8 \qquad (3\text{-}15)$$

3.3 Coolant Dynamics

Figure 4 is a schematic diagram showing the flows and terminal pressures needed for coolant dynamic simulation of the EBR-II primary system. EBR-II has a partitioned core. The inner core region, consisting of fuel, inner blanket, control and safety subassemblies, is fed by flow ($W_{C(i)}$) from the high pressure (HP) plenum. The outer core region, comprising the outer

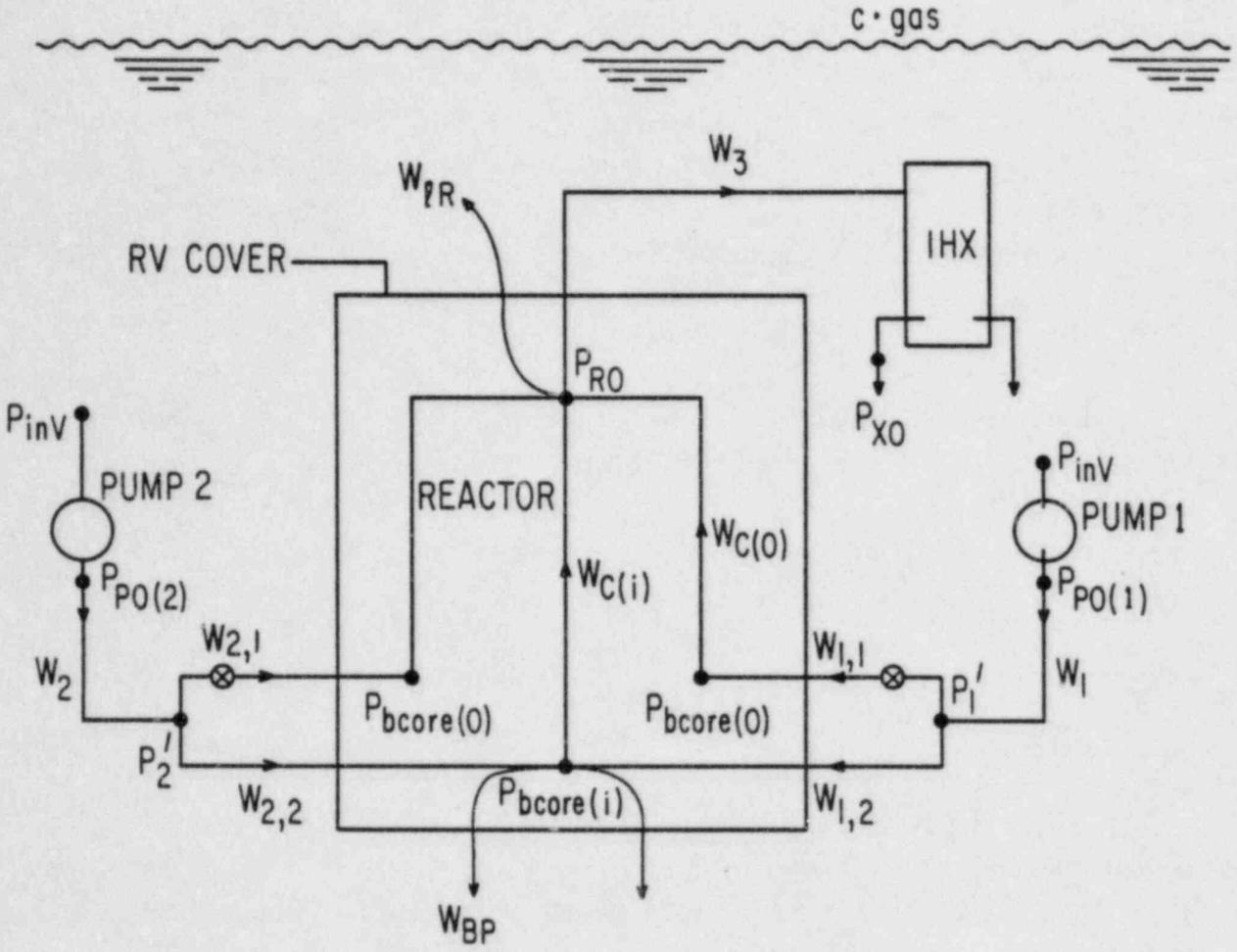

Fig. 4 Primary System Profile for Coolant Dynamics

blanket subassemblies, is fed by sodium flow ($W_{C(o)}$) from the low pressure (LP) plenum. The inner core region can be represented by one or more channels, with inter-channel flow redistribution being governed by buoyancy and frictional effects between $P_{bcore(i)}$ and P_{Ro}. Likewise, the outer core region can be represented by one or more channels, with inter-channel flow redistribution being governed by buoyancy and frictional effects between $P_{bcore(o)}$ and P_{Ro}. The flow split between the inner and outer regions is, of course, governed by overall primary coolant dynamics.

3.3.1 Leakage Flows

Leakage through the grid plenum assembly into the bulk pool sodium is essentially confined to the flow from the high pressure plenum [2]. Hence, for hydraulic modeling, W_{BP} will be located there (see Fig. 4). Also, leakages at pump disconnects ($W_{\ell P}$) and at throttling valve inlets ($W_{\ell V}$) which are a little over 10% of W_{BP} and occur at about the same pressure and temperature as the grid plenum leakage are lumped into W_{BP}. Thus,

$$W_{BP} = W_{BP} + W_{\ell P} + W_{\ell V} \tag{3-16}$$

There is also leakage past the reactor cover, flange, etc. ($W_{\ell R}$) into the cold pool. Leakage at the IHX inlet ($W_{\ell X}$), which is limited to 30 gpm at full flow conditions, is lumped with $W_{\ell R}$ to simplify the analysis. This should not affect the accuracy of the solution since leakage at IHX inlet is at essentially the same pressure and temperature as that past the reactor cover. Thus,

$$W_{\ell R} = W_{\ell R} + W_{\ell X} \tag{3-17}$$

3.3.2 System Flow Equations

The flow rates and terminal pressures are indicated in Fig. 4. Volume-averaged momentum equations can be written relating the rate of change of mass flow rate to the terminal pressures and losses in a uniform mass flow rate section. These are written below.

Flow at discharge of pump 1:

$$\frac{dW_1}{dt} \sum_{1} \left(\frac{L}{A}\right) = P_{Po(1)} - P'_1 - \sum_{1} \Delta P_{f,g} \qquad (3\text{-}18)$$

Flow through LP piping 1:

$$\frac{dW_{1,1}}{dt} \sum_{1,1} \left(\frac{L}{A}\right) = P'_1 - P_{bcore(o)} - \sum_{1,1} \Delta P_{f,g} \qquad (3\text{-}19)$$

Flow through HP piping 1

$$\frac{dW_{1,2}}{dt} \sum_{1,2} \left(\frac{L}{A}\right) = P'_1 - P_{bcore(i)} - \sum_{1,2} \Delta P_{f,g} \qquad (3\text{-}20)$$

Similarly, from pump 2 onward:

$$\frac{dW_2}{dt} \sum_{2} \left(\frac{L}{A}\right) = P_{Po(2)} - P'_2 - \sum_{2} \Delta P_{f,g} \qquad (3\text{-}21)$$

$$\frac{dW_{2,1}}{dt} \sum_{2,1} \left(\frac{L}{A}\right) = P'_2 - P_{bcore(o)} - \sum_{2,1} \Delta P_{f,g} \qquad (3\text{-}22)$$

$$\frac{dW_{2,2}}{dt} \sum_{2,2} \left(\frac{L}{A}\right) = P'_2 - P_{bcore(i)} - \sum_{2,2} \Delta P_{f,g} \qquad (3\text{-}23)$$

Flow through inner reactor region:

$$\frac{dW_{C(i)}}{dt} \sum_{c,i} \left(\frac{L}{A}\right) = P_{bcore(i)} - P_{Ro} - \sum_{c,i} \Delta P_{f,g} \qquad (3\text{-}24)$$

Flow through outer blanket assemblies:

$$\frac{dW_{C(o)}}{dt} \sum_{c,o} \left(\frac{L}{A}\right) = P_{bcore(o)} - P_{Ro} - \sum_{c,o} \Delta P_{f,g} \qquad (3\text{-}25)$$

Flow through IHX $W_3 (=W_X)$:

$$\frac{dW_3}{dt} \sum_{3} \left(\frac{L}{A}\right) = P_{Ro} - P_{Xo} - \sum_{3} \Delta P_{f,g} \qquad (3\text{-}26)$$

Some of the terminal pressures and flow rates can be obtained from algebraic equations.

From fluid statics, pump inlet-pressure P_{Pin} $(=P_{inV})$ is

$$P_{inV} = P_g + \rho_{CP}\, g\, (z_{CP} - z_{Pin}) \qquad (3\text{-}27)$$

The pressure at exit of pump 1 is obtained from

$$P_{Po(1)} = P_{inV} + \Delta P_{P(1)} \qquad (3\text{-}28)$$

where the pump pressure rise $\Delta P_{P(1)}$ is related to its head (H_1) obtained from the pump model by

$$\Delta P_{P(1)} = \rho_{CP}\, g\, H_1 \qquad (3\text{-}29)$$

Similarly, for pump 2

$$P_{Po(2)} = P_{inV} + \Delta P_{P(2)} \tag{3-30}$$

where

$$\Delta P_{P(2)} = \rho_{CP}\, g\, H_2 \tag{3-31}$$

Mass conservation at the branches downstream of pumps yields

$$W_1 = W_{1,1} + W_{1,2} \tag{3-32}$$

$$W_2 = W_{2,1} + W_{2,2} \tag{3-33}$$

Mass conservation at the HP plenum yields,

$$W_{C(i)} = W_{1,2} + W_{2,2} - W_{BP} \tag{3-34}$$

And, at the LP plenum

$$W_{C(o)} = W_{1,1} + W_{2,1} \tag{3-35}$$

At the reactor outlet plenum (pressurized, no free surface):

$$W_3 = W_{C(i)} + W_{C(o)} - W_{\ell R} \tag{3-36}$$

The steady-state leakage flow rate information can be utilized to write the following algebraic equations to determine transient leakage rates;

$$P_{bcore(i)} - P_{CP(i)} = \frac{K_{BP}\, W_{BP}^2}{\rho_{Rin}} \tag{3-37}$$

$$P_{Ro} - P_{CP(Ro)} = \frac{K_{\ell R} W_{\ell R}^2}{\rho_{Ro}} \qquad (3\text{-}38)$$

where K_{BP} and $K_{\ell R}$ are determined from steady-state pressures and leakage rates, and held constant during transient calculations.

In Eqs. (3-37) and (3-38), the pressures within the cold pool at the reactor HP inlet elevation, $P_{CP(i)}$, and over the reactor vessel cover, $P_{CP(Ro)}$, are obtained from fluid statics:

$$P_{CP(i)} = P_g + \rho_{CP}\, g\, (z_{CP} - z_{Rin}) \qquad (3\text{-}39)$$

$$P_{CP(Ro)} = P_g + \rho_{CP}\, g\, (z_{CP} - z_{Ro}) \qquad (3\text{-}40)$$

where z_{Rin}, z_{Ro} are the elevations at the reactor inlet and over the vessel cover, respectively.

The IHX exit pressure is also obtained from fluid statics as:

$$P_{Xo} = P_g + \rho_{CP}\, g\, (z_{CP} - z_{Xo}) \qquad (3\text{-}41)$$

In Eqs. (3-27), (3-39), (3-40) and (3-41) the cold pool level, z_{CP}, is needed. This is obtained dynamically from mass balance in the pool:

$$A_{cg} \frac{d}{dt} (\rho_{CP}\, z_{CP}) = W_3 - (W_1 + W_2) + W_{BP} + W_{\ell R} \qquad (3\text{-}42)$$

3.3.3 Channel Flows

Since the reactor coolant channels form part of the system flow circuits, their details need to be included in the coolant dynamic analysis of the primary system.

If N_{ch} is the number of channels simulated in the core, then

$$N_{ch} = N_{ch(i)} + N_{ch(o)} \tag{3-43}$$

The total flow through the inner and outer core regions can be written in terms of channel flows as

$$W_{C(i)} = \sum_{j=1}^{N_{ch(i)}} W_j \tag{3-44}$$

$$W_{C(o)} = \sum_{j=1}^{N_{ch(o)}} W_j \tag{3-45}$$

Differentiating both sides of Eqs. (3-44) and (3-45) we obtain

$$\frac{dW_{C(i)}}{dt} = \sum_{j=1}^{N_{ch(i)}} \frac{dW_j}{dt} \tag{3-46}$$

$$\frac{dW_{C(o)}}{dt} = \sum_{j=1}^{N_{ch(o)}} \frac{dW_j}{dt} \tag{3-47}$$

For each inner core channel j we can write, from momentum balance:

$$\frac{dW_j}{dt}\left(\sum \frac{L}{A}\right)_j = P_{bcore(i)} - P_{Ro} - \left(\sum \Delta P_{f,g}\right)_j \tag{3-48}$$

And, for each outer channel j:

$$\frac{dW_j}{dt}\left(\sum \frac{L}{A}\right)_j = P_{bcore(o)} - P_{Ro} - \left(\sum \Delta P_{f,g}\right)_j \tag{3-49}$$

3.3.4 Core Bypass Flow

If we consider the flow through clearances between assemblies, mainly in the inner core region (~120 gpm at full flow), to be lumped into a bypass flow associated with the inner core region (W_{BPi}), we can write the following equations:

$$\frac{dW_{C(i)}}{dt} = \sum_{j=1}^{N_{ch(i)}} \frac{dW_j}{dt} + \frac{dW_{BPi}}{dt} \qquad (3\text{-}50)$$

$$\frac{dW_{BPi}}{dt} \sum_{BPi} \left(\frac{L}{A}\right) = P_{bcore(i)} - P_{Ro} - \sum_{BPi} \Delta P_{f,g} \qquad (3\text{-}51)$$

3.3.5 Equations for Terminal Pressures

The integration of the system flow equations requires the terminal pressures to be determined explicitly using algebraic equations. These are derived as explained in the rest of this section.

Differentiating Eq. (3-34) for mass conservation at HP plenum, and neglecting the effect, if any, of changes in leakage flow (i.e., W_{BP}) to the cold pool, we get

$$\frac{dW_{C(i)}}{dt} = \frac{dW_{1,2}}{dt} + \frac{dW_{2,2}}{dt} \qquad (3\text{-}52)$$

The derivatives of $W_{1,2}$, $W_{2,2}$ above can be replaced by algebraic expressions involving terminal pressures and losses using Eqs. (3-20) and (3-23). Likewise, the derivative of $W_{C(i)}$ can be replaced by algebraic expressions involving terminal pressures using Eqs. (3-49), (3-50) and (3-51). Thus, Eq. (3-52) is rewritten as

$$\sum_{j=1}^{N_{ch(i)}} \frac{P_{bcore(i)} - P_{Ro} - \sum \Delta P_{f,g}{}_j}{\left(\sum \frac{L}{A}\right)_j} + \frac{P_{bcore(i)} - P_{Ro} - \sum_{BPi} \Delta P_{f,g}}{\sum_{BPi} \frac{L}{A}} =$$

$$\frac{P_1' - P_{bcore(i)} - \sum_{1,2} \Delta P_{f,g}}{\sum_{1,2} \frac{L}{A}} + \frac{P_2' - P_{bcore(i)} - \sum_{2,2} \Delta P_{f,g}}{\sum_{2,2} \frac{L}{A}} \qquad (3\text{-}53)$$

Equation (3-53) can be written in a more general form, suitable for matrix operations, as

$$a_{11} P_1' + a_{12} P_2' + a_{13} P_{bcore(i)} + a_{14} P_{bcore(o)} + a_{15} P_{Ro} = C_1 \qquad (3\text{-}54)$$

Here,

$$a_{11} = -\frac{1}{\sum_{1,2} \frac{L}{A}} \qquad (3\text{-}55)$$

$$a_{12} = -\frac{1}{\sum_{2,2} \frac{L}{A}} \qquad (3\text{-}56)$$

$$a_{13} = \sum_{j=1}^{N_{ch(i)}} \frac{1}{\left(\sum \frac{L}{A}\right)_j} + \frac{1}{\sum_{BPi} \frac{L}{A}} + \frac{1}{\sum_{1,2} \frac{L}{A}} + \frac{1}{\sum_{2,2} \frac{L}{A}} \qquad (3\text{-}57)$$

$$a_{14} = 0 \tag{3-58}$$

$$a_{15} = - \sum_{j=1}^{N_{ch(i)}} \frac{1}{\left(\sum \frac{L}{A}\right)_j} - \frac{1}{\sum_{BPi} \frac{L}{A}} \tag{3-59}$$

$$C_1 = \sum_{j=1}^{N_{ch(i)}} \frac{\left(\sum \Delta P_{f,g}\right)_j}{\left(\sum \frac{L}{A}\right)_j} + \frac{\sum_{BPi} \Delta P_{f,g}}{\sum_{BPi} \frac{L}{A}} - \frac{\sum_{1,2} \Delta P_{f,g}}{\sum_{1,2} \frac{L}{A}} - \frac{\sum_{2,2} \Delta P_{f,g}}{\sum_{2,2} \frac{L}{A}} \tag{3-60}$$

Differentiating Eq. (3-35) for mass balance at the LP plenum yields:

$$\frac{dW_{C(o)}}{dt} = \frac{dW_{1,1}}{dt} + \frac{dW_{2,1}}{dt} \tag{3-61}$$

In a similar manner, replacing all flow derivatives by algebraic expressions involving terminal pressures and rearranging, Eq. (3-61) is rewritten in the general form as:

$$a_{21} P_1' + a_{22} P_2' + a_{23} P_{bcore(i)} + a_{24} P_{bcore(o)} + a_{25} P_{Ro} = C_2 \tag{3-62}$$

where

$$a_{21} = - \frac{1}{\sum_{1,1} \frac{L}{A}} \tag{3-63}$$

$$a_{22} = -\frac{1}{\sum_{2,1} \frac{L}{A}} \tag{3-64}$$

$$a_{23} = C \tag{3-65}$$

$$a_{24} = \sum_{j=1}^{N_{ch(o)}} \frac{1}{\left(\sum \frac{L}{A}\right)_j} + \frac{1}{\sum_{1,1} \frac{L}{A}} + \frac{1}{\sum_{2,1} \frac{L}{A}} \tag{3-66}$$

$$a_{25} = -\sum_{j=1}^{N_{ch(o)}} \frac{1}{\left(\sum \frac{L}{A}\right)_j} \tag{3-67}$$

$$C_2 = \sum_{j=1}^{N_{ch(o)}} \frac{\left(\sum \Delta P_{f,g}\right)_j}{\left(\sum \frac{L}{A}\right)_j} - \frac{\sum_{1,2} \Delta P_{f,g}}{\sum_{1,1} \frac{L}{A}} - \frac{\sum_{2,1} \Delta P_{f,g}}{\sum_{2,1} \frac{L}{A}} \tag{3-68}$$

Differentiating Eq. (3-32) for mass conservation at branch 1, replacing flow derivatives using Eqs. (3-18), (3-19) and (3-20), and rearranging yields

$$a_{31} P_1' + a_{32} P_2' + a_{33} P_{bcore(i)} + a_{34} P_{bcore(o)} + a_{35} P_{Ro} = C_3 \tag{3-69}$$

$$a_{31} = -\left[\frac{1}{\sum_{1}\frac{L}{A}} + \frac{1}{\sum_{1,1}\frac{L}{A}} + \frac{1}{\sum_{1,2}\frac{L}{A}}\right] \tag{3-70}$$

$$a_{32} = 0 \tag{3-71}$$

$$a_{33} = \frac{1}{\sum_{1,2}\frac{L}{A}} \tag{3-72}$$

$$a_{34} = \frac{1}{\sum_{1,1}\frac{L}{A}} \tag{3-73}$$

$$a_{35} = 0 \tag{3-74}$$

$$C_3 = \frac{-P_{Po(1)} + \sum_{1}\Delta P_{f,g}}{\sum_{1}\frac{L}{A}} - \frac{\sum_{1,1}\Delta P_{f,g}}{\sum_{1,1}\frac{L}{A}} - \frac{\sum_{1,2}\Delta P_{f,g}}{\sum_{1,2}\frac{L}{A}} \tag{3-75}$$

Similarly, for branch 2, we obtain

$$a_{41} P_1' + a_{42} P_2' + a_{43} P_{bcore(i)} + a_{44} P_{bcore(o)} + a_{45} P_{Ro} = C_4 \tag{3-76}$$

where

$$a_{41} = 0 \tag{3-77}$$

$$a_{42} = -\left[\frac{1}{\sum_{2}\frac{L}{A}} + \frac{1}{\sum_{2,1}\frac{L}{A}} + \frac{1}{\sum_{2,2}\frac{L}{A}}\right] \tag{3-78}$$

$$a_{43} = \frac{1}{\sum_{2,2}\frac{L}{A}} \tag{3-79}$$

$$a_{44} = \frac{1}{\sum_{2,1}\frac{L}{A}} \tag{3-80}$$

$$a_{45} = 0 \tag{3-81}$$

$$C_4 = \frac{-P_{Po(2)} + \sum_{2}\Delta P_{f,g}}{\sum_{2}\frac{L}{A}} - \frac{\sum_{2,1}\Delta P_{f,g}}{\sum_{2,1}\frac{L}{A}} - \frac{\sum_{2,2}\Delta P_{f,g}}{\sum_{2,2}\frac{L}{A}} \tag{3-82}$$

The volume between pump outlets and IHX outlet is pressurized, with no free surface. Hence, mass flow through the heat exchanger is equal to the total flow through both pumps minus leakage flows. We can write mass conservation through the line as:

$$W_3 = W_1 + W_2 - W_{BP} - W_{\ell R} \tag{3-83}$$

Differentiating, and neglecting the effect of any changes in leakage rates (i.e., W_{BP} and $W_{\ell R}$), we obtain

$$\frac{dW_3}{dt} = \frac{dW_1}{dt} + \frac{dW_2}{dt} \tag{3-84}$$

Combining with Eqs. (3-26), (3-18) and (3-21), and rearranging yields the equation in terms of terminal pressures:

$$a_{51} P_1' + a_{52} P_2' + a_{53} P_{bcore(i)} + a_{54} P_{bcore(o)} + a_{55} P_{Ro} = C_5 \tag{3-85}$$

$$a_{51} = \frac{1}{\sum_1 \frac{L}{A}} \tag{3-86}$$

$$a_{52} = \frac{1}{\sum_2 \frac{L}{A}} \tag{3-87}$$

$$a_{53} = 0 \tag{3-88}$$

$$a_{54} = 0 \tag{3-89}$$

$$a_{55} = \frac{1}{\sum_3 \frac{L}{A}} \tag{3-90}$$

$$C_5 = \frac{P_{Po(1)} - \sum_1 \Delta P_{f,g}}{\sum_1 \frac{L}{A}} + \frac{P_{Po(2)} - \sum_2 \Delta P_{f,g}}{\sum_2 \frac{L}{A}} + \frac{P_{Xo} + \sum_3 \Delta P_{f,g}}{\sum_3 \frac{L}{A}} \qquad (3\text{-}91)$$

Equations (3-54), (3-62), (3-69), (3-76) and (3-85) form a system of simultaneous algebraic equations (along with equations for the constants), which can be solved by matrix inversion to obtain the terminal pressures P'_1, P'_2, $P_{bcore(i)}$, $P_{bcore(0)}$, and P_{Ro}.

3.3.6 Main Primary Pumps

The EBR-II main centrifugal pumps are single-stage units and are rated to deliver 0.34705 m^3/s (5500 gpm) of sodium at 60.96 m (200 ft.) total head and 1075 rpm [2]. This yields a rated specific speed $N_S \simeq 29$ (SI units) or 1500 (gpm units).

In the pump model developed for SSC-L [6], the impeller behavior is characterized by homologous head and torque relations encompassing all regions of operation. The homologous characteristics were derived from independent model test results with a centrifugal pump of specific speed $N_S = 35$ (SI units), and are applicable to LMFBR pumps in general. The model was shown to give very good agreement with measured data for FFTF pumps ($N_S \simeq 27.2$), and with vendor calculations for the CRBR pump ($N_S \simeq 42.8$). It is not anticipated therefore, that the characteristic coefficients built into the code will need to be changed for the EBR-II pumps with N_S within the same range.

Note that the high pressure piping from the pump contains no check valves, hence flow reversal here is a distinct possibility in case of asymmetric operation of the main pumps. EBR-II experience has shown that all four quadrants of pump operation may be involved in coastdown transients, depending on the type and sequence of power failure to the pumps [7]. This justifies the use of the 4-quadrant pump model in SSC for EBR-II simulation.

It is worth noting that each main centrifugal pump is driven by a separate motor-generator set through a variable-speed eddy-current clutch. As indicated in Figure 5, there is a 2400-V circuit breaker at the input to each M-G motor, a 110-V breaker in the eddy-current clutch between this motor and the generator, and a breaker at the input to each pump motor. Depending on the initiation signal, the power supply to the primary pumps can thus be interrupted in different modes (see Figure 5). It has been observed from measured data that the rate of flow decay following a loss of pumping power is dependent on the mode of power interruption [9].

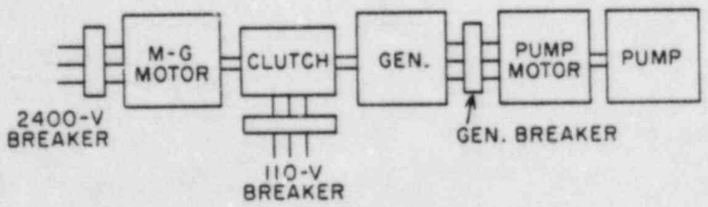

Figure 5. Schematic of Pump Drive Components [9]

A mathematical representation will therefore be required to account for the effect of the various modes of power interruption to the pumps. The code should also be able to accommodate different characteristics for the two main pumps.

3.3.7 Pressure Losses in Pipes

The pressure loss terms ($\Delta P_{f,g}$) in the flow equations discussed earlier represent the pressure losses in various pipe sections and are calculated as

$$\Delta P_{f,g} = \text{accel. loss} + \text{frictional loss} + \text{gravity loss (gain)} + \text{other losses.}$$

$$= W^2(1/\rho_N - 1/\rho_1)/A^2 + \frac{W|W|}{2DA^2}\int_0^L \frac{f}{\rho}\,dx + g\int_0^L \rho \sin\alpha\,dx + K\,W|W|/\bar{\rho}A^2 \qquad (3\text{-}92)$$

The various terms are clearly explained elsewhere [3]. K here is a coefficient to account for losses due to bends, fittings, etc. If the overall pressure drop across the pipe is known during steady-state, K can be evaluated easily, and remains constant during transient. If not known, K is estimated from physical data of the pipe, such as number and angle of bends, number and type of fitting, etc. This option is available in SSC. For the low pressure line, the pressure loss across the throttle valve is also lumped in this term. Based on data of pressure loss across the valve during full-flow, the contribution of the valve to overall K is evaluated.

The pressure rise across the auxiliary EM pump can, at present, be assumed constant at its steady-state value [8], until a better representation is developed. This term can be lumped together with the pressure loss terms for the reactor outlet piping.

4. PRIMARY SYSTEM DATA

4.1 Operating Data

Reactor

Inlet temperature	371.11	°C	(700°F)
Outlet temperature	472.78	°C	(883°F)
Power	62.3	MWt	

The above are measured values corresponding to Run 38A [2].

IHX

Most of the numbers below are measured values corresponding to Run 38A [2].

Primary flow (shell side)	480.05	kg/s (3.81×10^6 lb/hr)
Primary sodium inlet temperature	471.11	°C
Primary sodium outlet temperature	371.11	°C
Secondary flow (tube side)	297.35	kg/s (2.36×10^6 lb/hr)
Secondary sodium inlet temperature	307.78	°C
Secondary sodium outlet temperature	466.67	°C
Primary sodium pressure drop	23.44	kPa [14.5 kPa in Ref. 10]
Secondary sodium (predicted) pressure drop	19.305	kPa [24.1 kPa in Ref. 11]
LMTD [10]	27.3	°C

Main Primary Pumps [2]

The rated characteristic parameters are

Capacity Q_R = 0.34705 m^3/s (5500 gpm)

Speed N_R = 1075 rpm

Head H_R = 60.96 m

Total pump heat into cold pool during full flow operation = 255 kW.

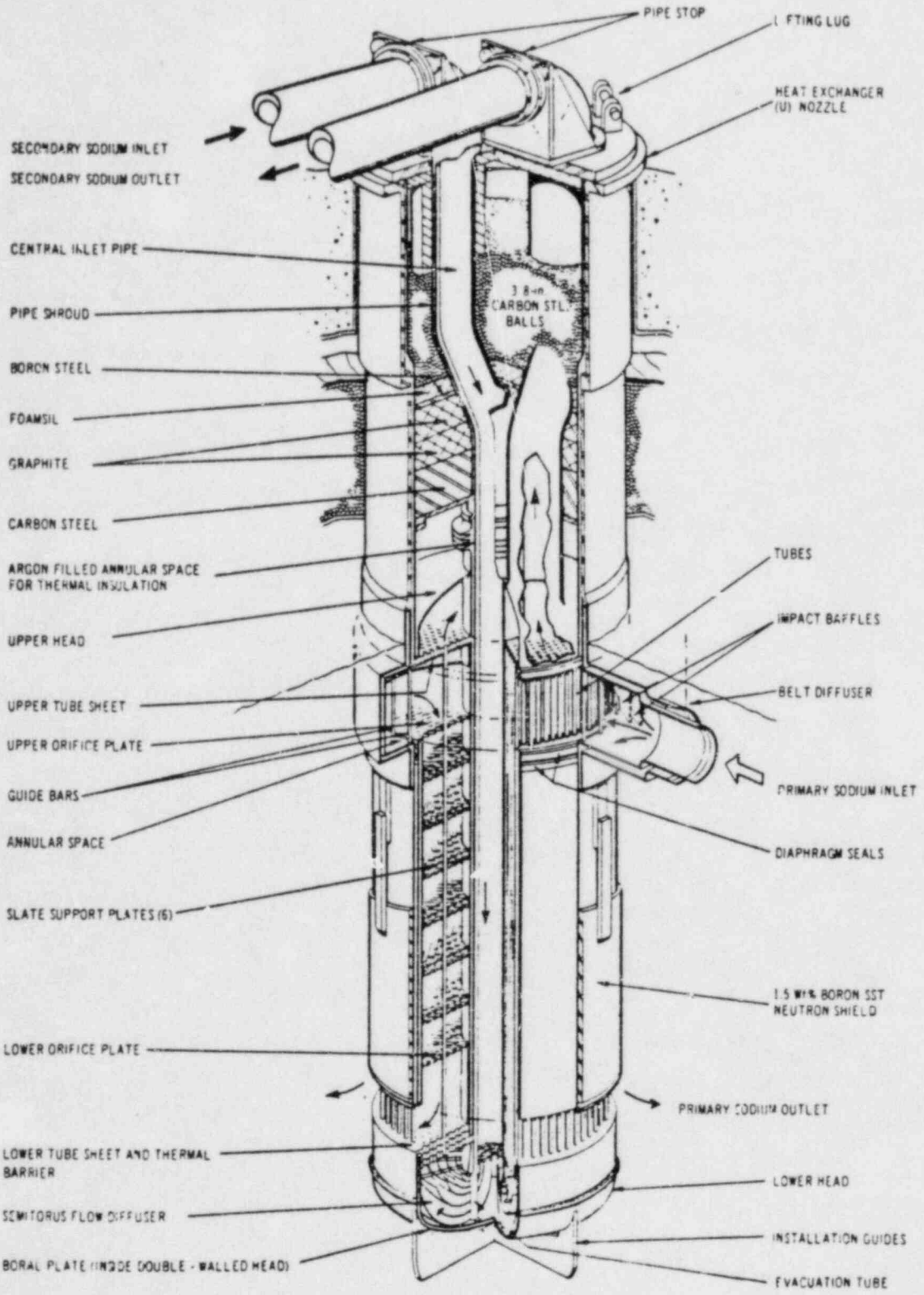

Fig. 6 Intermediate Heat Exchanger [15]

Coolant Flows

The values below have been converted to m^3/s from gpm values listed in Ref. 2 at 427°C (800°F).

Coolant flow from pumps		0.5894
Leakage at pump disconnects	0.631×10^{-3}	
Leakage at throttle valves	1.5775×10^{-3}	
Flow into reactor lower plena		0.5871
Leakages past inner core region	19.246×10^{-3}	
Flow through reactor		0.5679
Flow through inner core region	0.4808	
Flow through outer blanket assemblies	79.506×10^{-3}	
Leakage past reactor cover, etc.	6.626×10^{-3}	
Flow to IHX		0.5613
Leakage at IHX inlet	1.893×10^{-3}	
Flow through IHX		0.5594

Primary Sodium Inventory [2]

Cold pool	290752.7 kg
Reactor vessel	2268.0 kg
IHX primary side	1814.4 kg

Pressure Drops [2]

Pump outlet to reactor inlet (HP line)	19.305 kPa
Reactor inlet to HP plenum	9.653 kPa
HP plenum to reactor upper plenum	281.306 kPa
Upper plenum to reactor outlet nozzle	8.274 kPa
Reactor outlet nozzle to IHX inlet	44.126 kPa
LP plenum to reactor upper plenum	26.890 kPa
Throttle valve at full flow	255.106 kPa
Pump outlet to LP plenum	269.585 kPa

4.2 Dimensional Data

IHX [11]

Number of tubes	3026	
Tube outside diameter	15.9	mm
Tube wall thickness	1.3	mm (1.6 mm in Ref. 10)
Tube pitch (triangular)	20.6	mm
Tube length (overall)	3.16	m
Tube sheet thickness (upper & lower)	76.2	mm each
Heat transfer area (secondary)	367	m^2
Active length	2.8 2.94	m [10] m [2]

Reactor Outlet Pipe

The dimensions are shown in Fig. 7.

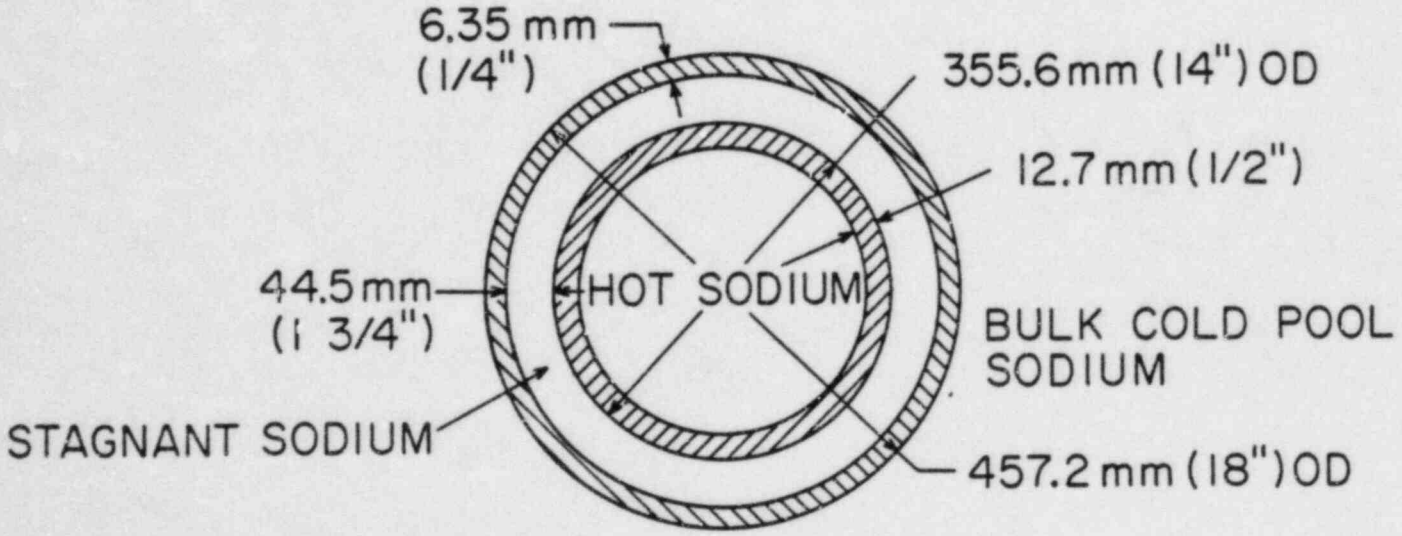

Fig. 7 Cross-section of Reactor Outlet Pipe

Primary System [2,12,13,14]

The dimensions are indicated in Figs. 8, 9. Some of the numbers have been obtained by measurements from a scale drawing in Ref. 2, and, hence this information should be taken as tentative, until confirmed data are obtained.

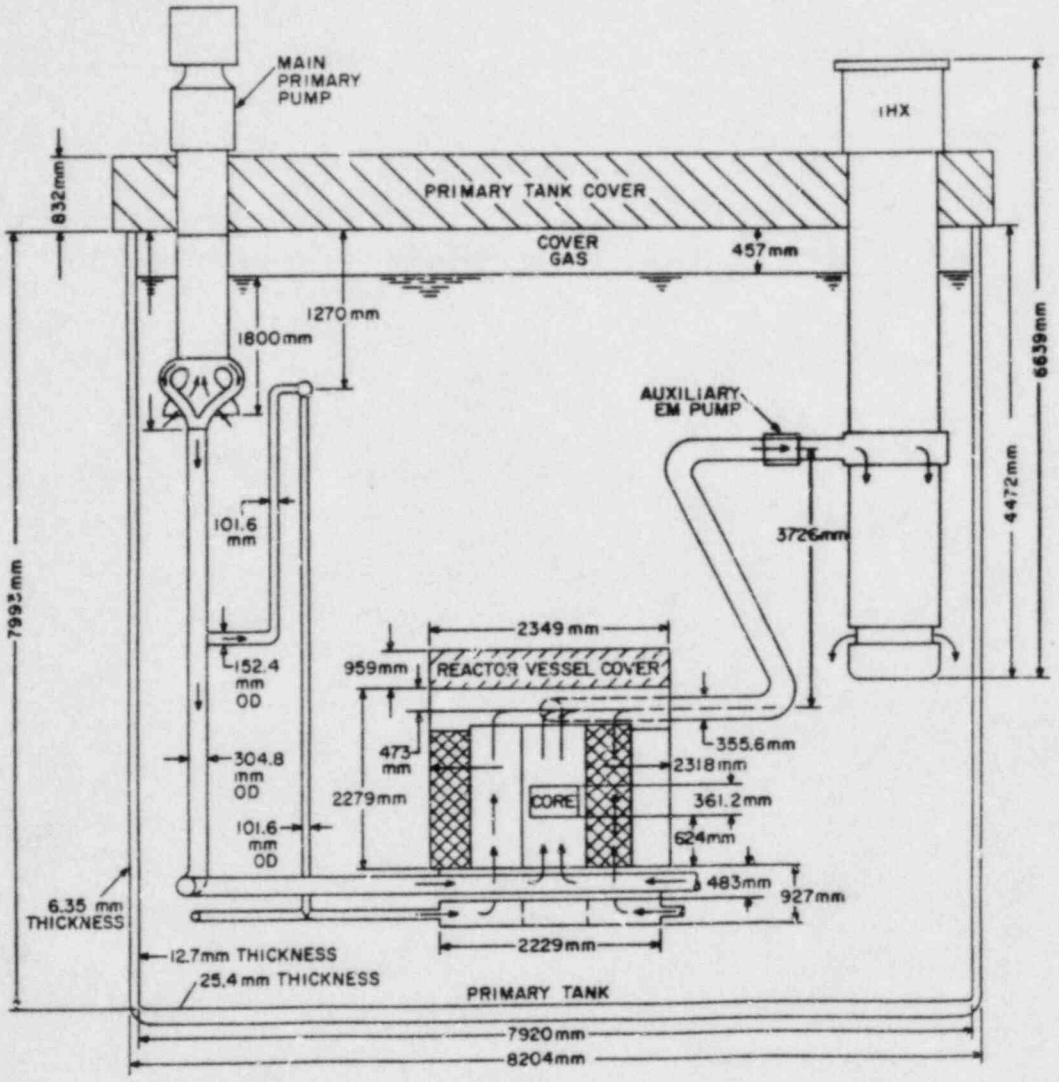

Fig. 8 Dimensional Data for Primary System

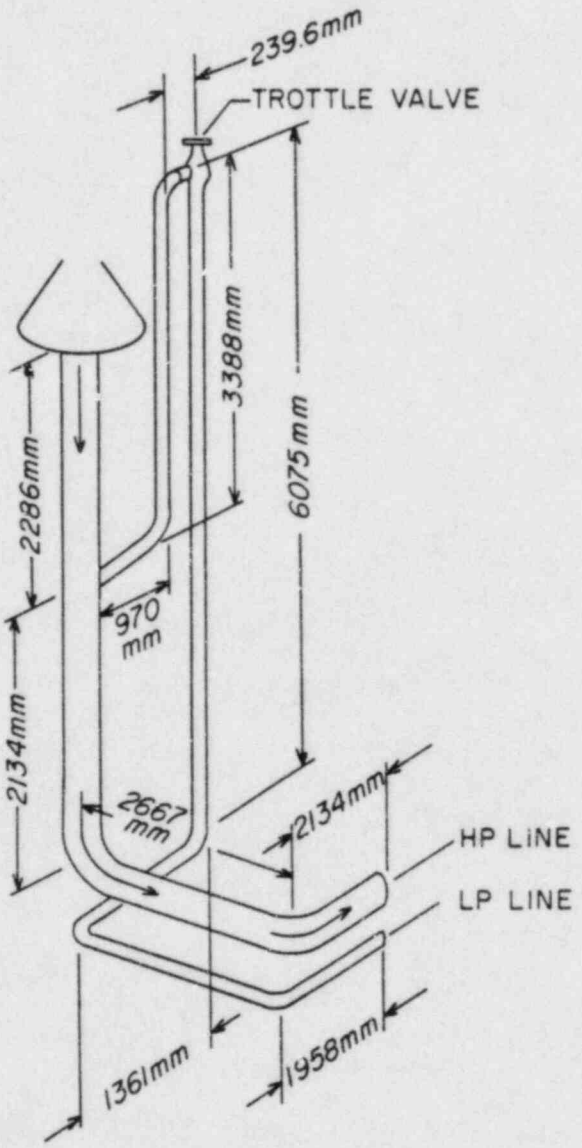

Fig. 9 Dimensional Data for Primary Cold Leg Piping

REFERENCES

1. J. G. Guppy, et al., "Super System Code (SSC, Rev. 0) An Advanced Thermo-hydraulic Simulation Code for Transients in LMFBRs", Brookhaven National Laboratory, BNL-NUREG-51650 (1983).

2. EBR-II System Design Description, Vol. III.

3. I. K. Madni, "Numerical Simulation of Thermal-hydraulic Transients in LMFBR Piping Systems," Numerical Heat Transfer, Vol. 6, 189 (1983).

4. Heat Transfer Data Book, General Electric Co., 1978.

5. I. K. Madni and E. G. Cazzoli, "An Advanced Thermohydraulic Simulation Code for Pool-Type LMFBRs (SSC-P Code)," Brookhaven National Laboratory, BNL-NUREG-51280 (1980).

6. I. K. Madni, E. G. Cazzoli, and A. K. Agrawal, "A Single-Phase Sodium Pump Model for LMFBR Thermal-Hydraulic Analysis," Proceedings of the International Meeting on Fast Reactor Safety Technology, Seattle, Washington, Aug. 19-23, 1979.

7. D. Mohr, "Final Report on NATCON," Argonne National Laboratory (1979).

8. L. J. Koch, et al., "Construction Design of EBR-II: An Integrated Unmoderated Nuclear Power Plant," International Conference on Peaceful Uses of Atomic Energy, Vol. 9, 1958.

9. D. Mohr and A. Gopalakrishnan," Coastdown Characteristics of the EBR-II Primary System," Trans. Am. Nucl. Soc. 17, (1973).

10. A. K. Agrawal and M. Khatib-Rahbar, "Dynamic Simulation of LMFBR Systems," Atomic Energy Review 18, 329 (1980).

11. H. W. Buschman, et al., "Design and Operating Experience of EBR-II Intermediate Heat Exchanger," ASME Paper No. 79-WA/NE-2.

12. J. Yevick, Fast Reactor Technology: Plant Design, M.I.T. Press, Cambridge, MA, 1966.

13. L. J. Koch, et al., "Hazard Summary Report, Experimental Breeder Reactor II (EBR-II)," Argonne National Laboratory, ANL-5719 (1957).

14. L. J. Koch, et al, "Addendum to Hazard Summary Report, Experimental Breeder Reactor II (EBR-II)," Argonne National Laboratory, ANL-5719 (Addendum) (1962).

15. L. J. Koch, "EBR-II: An Experimental LMFBR Power Plant," Reactor Technology, Vol. 14, No. 3, 286 (1971).

NRC FORM 335 (11-81)

U.S. NUCLEAR REGULATORY COMMISSION

BIBLIOGRAPHIC DATA SHEET

1. REPORT NUMBER (Assigned by DDC)
NUREG/CR-3878
BNL-NUREG-51797

4. TITLE AND SUBTITLE (Add Volume No., if appropriate)
Modeling Considerations for the Primary System of the Experimental Breeder Reactor-II

2. (Leave blank)

3. RECIPIENT'S ACCESSION NO.

7. AUTHOR(S)
I. K. Madni

5. DATE REPORT COMPLETED
MONTH: May YEAR: 1984

9. PERFORMING ORGANIZATION NAME AND MAILING ADDRESS (Include Zip Code)
Department of Nuclear Energy
Brookhaven National Laboratory
Upton, Long Island, New York 11973

DATE REPORT ISSUED
MONTH YEAR

6. (Leave blank)

8. (Leave blank)

12. SPONSORING ORGANIZATION NAME AND MAILING ADDRESS (Include Zip Code)
Division of Accident Evaluation
Office of Nuclear Regulatory Research
U.S. Nuclear Regulatory Commission
Washington, D.C. 20555

10. PROJECT/TASK/WORK UNIT NO

11. FIN NO.
A-3015

13. TYPE OF REPORT
Technical Report

PERIOD COVERED (Inclusive dates)

15. SUPPLEMENTARY NOTES

14. (Leave blank)

16. ABSTRACT (200 words or less)

This report describes the additional heat transfer and coolant dynamic models for components and processes, that are needed for simulation of the primary system of the Experimental Breeder Reactor-II (EBR-II). This work forms part of the Super System Code (SSC) application efforts to provide predictions of EBR-II overall plant behavior.

17. KEY WORDS AND DOCUMENT ANALYSIS

17a. DESCRIPTORS

Thermal/Hydraulic Analysis
Cold Pool, System Analysis
Transient Analysis
EBR-II System Representation
LMFBR

17b. IDENTIFIERS/OPEN-ENDED TERMS

18. AVAILABILITY STATEMENT
UNLIMITED

19. SECURITY CLASS (This report)
unclassified

21. NO. OF PAGES

20. SECURITY CLASS (This page)
unclassified

22. PRICE
$

NRC FORM 335 (11-81)